Computational fluid dynamics (CFD) modeling of grain-water suspensions in tube

Kanishka Bhunia, Ranjeet Kumar Sharma, A. K. Datta*

(Agricultural and Food Engineering Department Indian Institute of Technology Kharagpur West Bengal, India)

Abstract: In this study of solid-liquid flow, rice and cassava starch particles were used as the dispersed media and water was used as the carrier fluid. Experiments were carried out on slurries with solid concentrations of 5%, 10% and 15% w/w which flowed in a 13mm ID and 3 m long tube –in - tube heat exchanger. Steam was used as the heating medium. Calculated convective film to particle heat transfer coefficient (hfp) values ranged from 11 to 32 kW m^{-2} K^{-1} for cassava and rice particles with uncertainty of ± 2 kW m^{-2} K^{-1}. A decrease in heat transfer coefficient values was found as a result of short residence time at the higher flow rates. To investigate the solid-liquid two-phase flow Eulerian multiphase model was adopted in simple axisymmetric geometry. Velocity profiles of the liquid and solid phases with different particle fractions were estimated from the simulated results. The respective velocities of both phases were higher in the upper part of the tube than in the lower portion because of settling caused by gravity. The slip velocity of particles was estimated from the simulations and it ranged from 6.68 cm/s to 9.80 cm/s for the cassava particles and 13.83 cm/s to 19.38 cm/s for the rice particles. The rice grains always lagged the liquid phase where as the cassava starch globules moved faster than the carrier liquid in the central region and very close to the wall. The particle volume concentration profile was also investigated and it was observed that a high particle concentration formed a core around tube centreline.

Keywords: CFD, Eulerian, slip velocity, solid-liquid flow, heat transfer, numerical, modelling

Citation: Bhunia, Kanishka, Ranjeet Kumar Sharma and A. K. Datta. 2016. Computational fluid dynamics (CFD) modelling of grain-water suspensions in tube. Agric Eng Int: CIGR Journal, 18(1):269-283.

1 Introduction

Institutional cooking represents a very critical step in most of the food preparations for mass consumption. Industrial thermal processing brings about irreversible changes in food textural and sensory properties, whilst at the same time achieving the desired level of microbial sterility. Also, organoleptic and nutritive properties of foods are adversely affected by heat, and the process must only be as severe as necessary to ensure commercial sterility. So, the optimization of such thermal treatments poses to be very challenging to the manufacturer. The problem of optimizing such a process is difficult for single phase foods; it is even more intractable when nonhomogeneous highly-viscous foodstuffs bearing large solid food particulates are handled. Since the presence of solids with viscous carrier fluid makes the system complex in nature and due to lack of data on critical factors such as i) the residence time distribution (RTD) in the holding tube system, ii) the velocity distribution of solids over the tube cross-sectional area and iii) the fluid-to-particle heat transfer pattern, it is very difficult to accurately design the equipment for continuous aseptic processing of solid-liquid food flows. Thus, to design an equipment to achieve the desired level of sterilization without overcooking of the solid-liquid food under a continuous system, the knowledge of fluid-to-particle heat transfer is necessary. Accurate application of this knowledge makes the process economical also. The residence time of any suspension is also important to get a desired level of sterilization which is influenced by nature and the velocity distribution of individual phase flowing through the tube. So, the velocity magnitudes and the velocity profiles of the solid must be used as guide to designing the process equipment. Mathematical modelling provides good

Received date: 2015-07-20 **Accepted date:** 2015-11-23
***Corresponding author: A. K. Datta,** akdiitkgp@gmail.com, Phone: +91-3222-283118, Fax: +91-3222-255303

insight into the process of heat transfer from fluid-to-particle over a considerable range that helps in determining the required heat to be supplied without conducting experiment.

Dutta and Sastry (1990a; 1990b) used videotaping to resolve the velocity distribution of polystyrene spheres and found that under low viscosity condition the fastest particle velocities were less than the centre line velocity of the fluid, but at higher viscosities the centreline velocity was exceeded. Liu et al.(1992) reported the work on horizontal food flow up to 30% solid concentration in water and other fluids. Tucker and Withers (1994) studied the effects of flow rates and particle concentrations on RTDs in starch suspensions. Kelly et al. (1995) used the stationary and moving thermocouple experimental techniques to simulate the heat transfer between a fluid and a particle in tube flow using water and carboxymethylcellulose (CMC) solutions. The fluid viscosity was found to significantly affect h_{fp}; an increase in the fluid viscosity decreased the value of h_{fp}. Also it was found that the increase in the particle size within the tube flow increased h_{fp} while particle shape had little effect on h_{fp}. A dimensionless Nusselt correlation was also obtained in terms of the generalized Reynolds and Prandtl numbers for both Newtonian and non-Newtonian fluids. Baptista et al. (1997) determined the average fluid-to-particle heat transfer coefficient for spherical aluminium particles with CMC as a carrier fluid for stationary and rotating particle. The obtained results were compared with published correlation and Frössling type relation ($Nu = Nu_0 + a\ Re^{\ b}\ Pr^{\ c}$) was found to be adequate to predict the value for a particular particle Reynolds number range. Mankad et al.(1997) evaluated the fluid to particle convective film heat transfer coefficient (h_{fp}) value for varying solid fractions and obtained data which compared well with published correlations. They found that Ranz-Marshal (1952) correlation was better predictor for single particle system. However, at reduced voidage Agarwal's (1988) correlation, based on accurate single-particle data, proved to be more successful in predicting h_{fp}. Ramaswamy and Zareifard (1999) successfully developed dimensionless correlations for particle oscillatory motion and calorimetric approach to predict the h_{fp} values. They also expressed Nusselt number as a function of Prandtl number and Reynolds number. Fluid-to-particle heat transfer for spherical particles (green peas) and carrier fluid (CMC) in continuous tube flow by means of pumping in coiled and straight tube heat exchanger was reported by Singh and Chakrabandhu (2002). The total system was portrayed as a packed bed. They found that h_{fp} value increased with temperature, flow rate, and particle concentration. The principal objective of the work being reported here was to develop a model describing fluid-to-particle heat transfer coefficient with water – cassava/rice suspension while flowing through concentric double tube heat exchanger. The specific objectives of the study were: i) to determine the effects of particle shape and size on heat transfer coefficient; ii) to determine wall-to-fluid and fluid-to-particle film heat transfer coefficients; iii) to investigate the flow patterns of solid particles using Computational Fluid Dynamics (CFD) for continuous tube flow; and iv) to develop a model describing fluid-to-particle film heat transfer coefficient. Krampa-Morlu et al. (2004) used computational fluid dynamics (CFD) to study the flow features of coarse aqueous solid–liquid slurries in turbulent upward flow including velocity profiles. They implemented the commercial CFD software CFX4.4 (ANSYS Inc.), and the simulation was carried out using experimental data from Sumner et al. (1990). The particles had density of 2650 kg/m^3 and diameter of 1.7 mm and were simulated at concentrations up to 30% v/v. The authors concluded that, using the default settings, the code failed to accurately predict important features of the flow. Eesa and Barigou (2008) investigated the flow of coarse, near-neutrally buoyant particles in shear-thinning CMC fluids in a horizontal pipe for a small number of flow cases by CFD. They found that CFD results of particle velocity profiles

were validated using experimental data obtained by PEPT (Positron emission particle tracking).

Eesa and Barigou (2009) investigated the laminar pipe transport of coarse particles in non-Newtonian carrier fluids of the power law type using an Eulerian – Eulerian computational fluid dynamics (CFD) model. They studied the flow with varying particle diameters (2–9 mm), mean solids concentrations (5%–40% v/v), mean suspension velocities (25–125 mm/s), and rheological properties of the carrier fluid (k = 0.15–20 Pa-s^n ; n = 0.6–0.9).

Based on the chronological evolution in the field of experimental determination and computational estimations of heat transfer coefficients, the research gap, as evident from the cited literature is the need to apply mathematical modelling and computational fluid dynamics to process equipment, commissioned with the specific objectives of bacterial inactivation and preservation of nutrients. Accurate estimations of dimensionless numbers and subsequent computation of heat transfer coefficients would lead to optimal design of process machineries. Specific objectives of the present study were:

i) Determination of wall-to-fluid and fluid-to-particle film heat transfer coefficient for grain-water suspension.

ii) Development of velocity profiles of the grain particles and the carrier liquid using Computational Fluid Dynamics (CFD) for continuous tube flow.

2 Materials and methods

Badsha bhog rice (8% moisture content on wet basis, 18% brokens and 600 kg/m^3 bulk density) and Cassava (1 – 2 mm diameter spheres of 2-3% moisture content on wet basis) starch procured from the local market were incorporated as solid food particles in water, which was the carrier fluid. A tube-in-tube heat exchanger with 13 mm internal and 22 mm outside diameter and 3 m length was used in Dairy and Food Engineering laboratory of Agricultural and Food Engineering Department of Indian Institute of Technology Kharagpur. Through the inside of the tube the solid-liquid suspension was allowed to pass by means of pumping. The heat exchanger was connected to a boiler from which hot steam was supplied as heating medium. A stirrer was immersed in the suspension to make the latter uniform throughout the duration of the experiment and it did not allow particles to settle down in the tank. A strainer with a thermocouple was kept just at the exit of the heat exchanger to collect the bulk solid material to gauge the average temperature of the solid particles. Also two thermocouples were attached at the inlet and the outlet of the heat exchanger which sensed the temperatures of the steam and the liquid at the outlet. The solid-liquid suspension was flowing through the heat exchanger in which steam was used as the heating medium. So, at first heat was transferred to the liquid and then to the particles. A simple steady state heat transfer equation was adopted to calculate wall-to-liquid heat transfer coefficient.

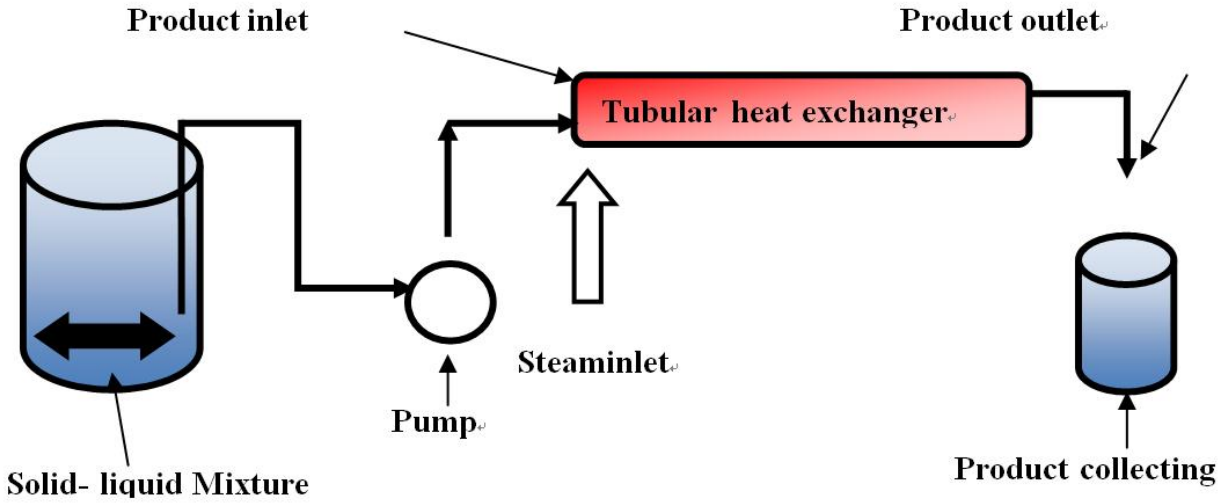

Figure1 Schematic diagram of experimental setup for the h_{fp} experiment

This equation is as follows:

$$hA_i\Delta T_{lm} = Q\rho_s(1-\varphi)C_{pw}\Delta T_w \quad (1)$$

Steady state heat transfer equation was also used to calculate fluid to particle film heat transfer coefficient.

$$h_{fp}A_p\Delta T = Q\rho_s\varphi C_{pg}\Delta T_g \quad (2)$$

CFD Simulations were setup in two dimensions using the commercial software package GAMBIT 2.4.6. Practically the geometry used here consisted of a pipe of inside diameter *D* = 13mm and the horizontal straight pipe length, L= 3m which is much greater than the maximum entrance length, L_e, required for flow to be fully developed. In single-phase Newtonian laminar flow, L_e can be estimated from

$$\frac{L_e}{D} = 0.062Re_t \quad (3)$$

However, given the fact that the particles considered here were non-neutrally buoyant, the above correlation for single phase flow would be expected to give a reasonable estimate of L_e.. A number of numerical experiments were conducted with different pipe lengths. At lower values Re_t (<2000), a pipe length of 600 mm was sufficient to give fully developed flow of the suspensions considered whilst keeping computational cost low. Using a longer pipe did not affect the two-phase pressure gradient or the velocity profile of either phase. At higher Re_t values, a length of 2000 mm was used (Eesa and Barigou, 2008).

The geometry was meshed in to 15000 quadrilateral cells with 30530 faces and 15531 nodes. Slip Reynolds number is given by:

$$Re_s = \frac{\rho_f D_p|v_f - v_p|}{\mu_f} \quad (4)$$

The simplest "complete models" of turbulence are two-equation models in which the solution of two separate transport equations allows the turbulent velocity and length scales to be independently determined. The standard $k-\epsilon$ model is a semi-empirical model based on model transport equations for the turbulence kinetic energy (k) and its dissipation rate (ϵ). The model transport equation for k is derived from the exact equation, while the model transport equation for ϵ was obtained using physical reasoning and bears little resemblance to its mathematically exact counterpart. In the derivation of the $k-\epsilon$ model, the assumption is that the flow is fully turbulent, and the effects of molecular viscosity are negligible. The standard $k-\epsilon$ model is therefore valid only for fully turbulent flows.

The turbulent kinetic energy k in J and its rate of dissipationϵin J is obtained from the following transport equations:

$$\frac{\delta}{\delta t}(\rho k) + \frac{\delta}{\delta x_i}(\rho k v_i) = \frac{\delta}{\delta x_j}[(\mu + \frac{\mu_t}{Pr_k})\frac{\delta k}{\delta x_j}] + G_k + G_b - \rho\epsilon - Y_M + S_k \quad (5)$$

and

$$\frac{\delta}{\delta t}(\rho\epsilon) + \frac{\delta}{\delta x_i}(\rho\epsilon v_i) = \frac{\delta}{\delta x_j}\left[\left(\mu + \frac{\mu_t}{Pr_\epsilon}\right)\frac{\delta\epsilon}{\delta x_j}\right] + H_{1\epsilon}\frac{\varepsilon}{k}($$

$$G_k + H_{3\epsilon}G_b) - H_{2\epsilon}\rho\frac{\epsilon^2}{k} + S_\epsilon \quad (6)$$

3 Results and discussion

3.1 Wall to liquid heat transfer coefficient

The heat balance equation described in Equation 1 was used to calculate wall to liquid heat transfer coefficient (h).

3.1.1 Wall to liquid heat transfer coefficient for cassava starch suspension

Figure 2 shows wall to liquid heat transfer coefficients (h) for 5%, 10%, 15% (w/w) particle fractions of cassava starch globules in water. The highest and the lowest values were 3.32, 2.86; 3.10, 2.89 and 2.47, 2.24 kW m^{-2} K^{-1} for 5%, 10% and 15% w/w solid fractions respectively. The figures clearly show the decrease in heat transfer coefficient with incrase in flow rates. This emphasizes heat transfer coefficient was decreasing with decrease in residence time of suspension in the holding tube as well as larger mass to be heated. As the suspension flow rate increased, the residence time of larger quantity of fluid flowing through the tube decreased resulting in decrease in fluid temperature at the outlet.

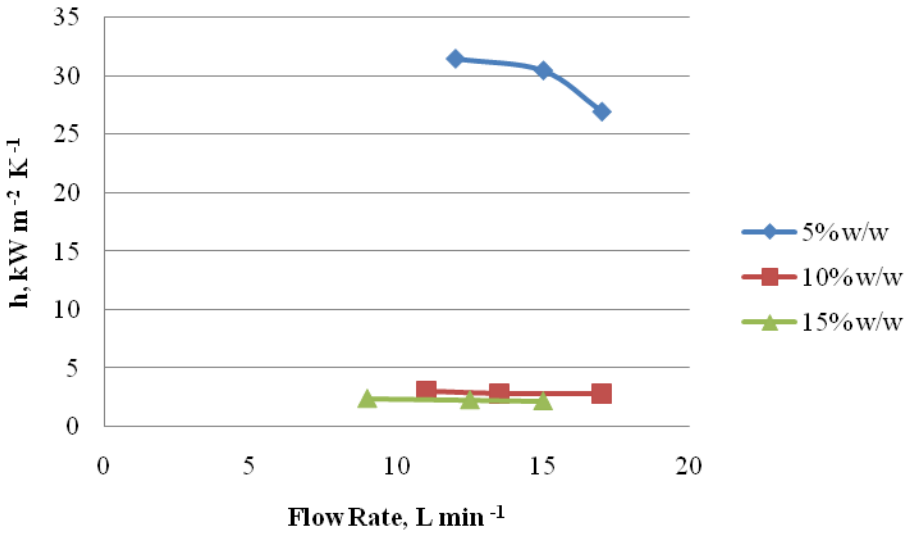

Figure 2 Plots of h values against flow rates of cassava-water suspension for different solid fractions

3.1.2 Wall to liquid heat transfer coefficient for rice suspension

Similar patterns were achieved for rice suspension also. The highest and the lowest values were 3.30, 2.84; 3.05, 2.85 and 2.43, 2.20 kW m^{-2} K^{-1} for 5%, 10% and 15% w/w solid fractions respectively. Here also convective film heat transfer coeficient (h) decreased with increasing flow rate as the residence time was very short for larger quantity of fluid. Figure 3 shows clearly the decrease in heat transfer coefficient with increase in the flowrate.

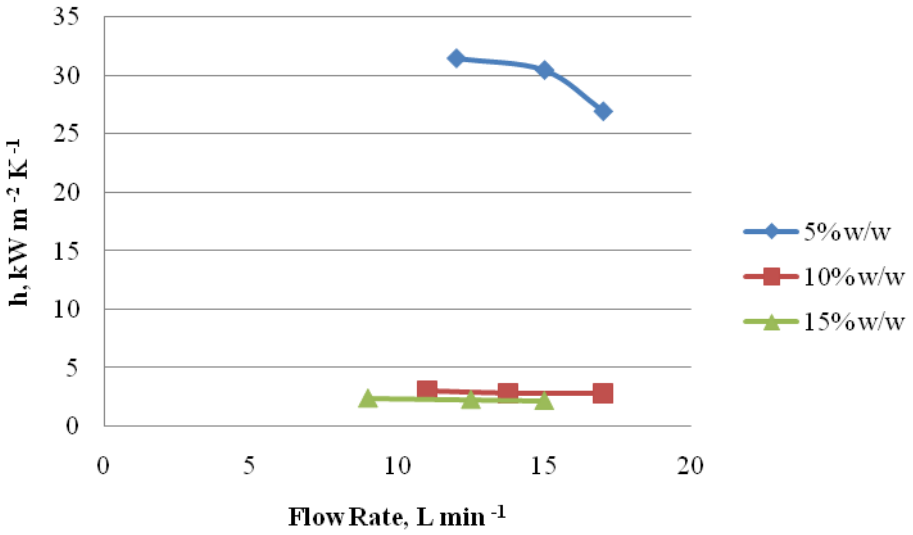

Figure 3 Plots of h values against flow rates of rice-water suspension for different solid fractions

3.2 Fluid-to-particle heat transfer coefficient

3.2.1 Fluid-to-particle heat transfer coefficient for cassava suspension

Fluid-to-particle heat transer coefficient (h_{fp}) was obtained using Equation (2). Figure 4 shows that higher value of 32 kW m^{-2} K^{-1} was obtained for 5% cassava suspension and the lower value is 11 kW m^{-2} K^{-1} for 15% cassava suspension.

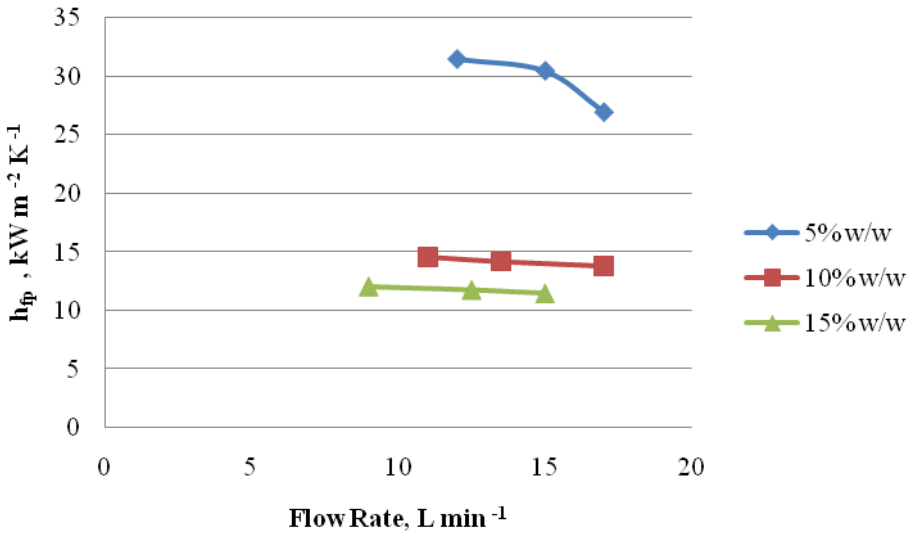

Figure 4 Plots of h_{fp} values against flow rates of cassava-water suspension for different solid fractions

The downward slope of the curve for each particular solid fraction indicates larger quantity heated in shorter exposure time in the holding tube as the suspensionflow rate increases. The heat transfer coefficient was high because of the very small particle size of cassava granule of about 1.562mm diameter. The temperature of the particle was about 59 ℃ when liquid temperature was 60 ℃. So, heat transfer was very high during this short residence time. The surface area of a single cassava globule was found out as 7.66 mm^2. At lower delivered solid fraction, mass of particles present in the flow system was also low which resulted in greater heat source to sink mass ratio. So, temperature of the fluid and the particle rose in a good manner resulting in relatively low temperature gradient between the fluid and the particle. As the particle concentration increased, the passage of the

fluid flow decreasedresulting in lower heat source to sink mass ratio. This turbulence, thus generatedretarded the temperature rise ofthe particlesas well as resulting in lower values of fluid-to-particle heat transer coefficient (h_{fp}), mainly due to greater temperature gradient between the fluid and the particle.

3.2.2 Fluid-to-particle heat transfer coefficient for rice suspension

Quite similar values were obtained for 5% rice suspension as those of 5% cassava suspension as shown in Figures 5. The highest value obtained was 32 kW m^{-2} K^{-1} for 5% rice suspension and the lower value was obtained as 11 kW m^{-2} K^{-1} for 15% w/w solid fraction. This again describes the similar kind phenomennon as of cassava suspension.

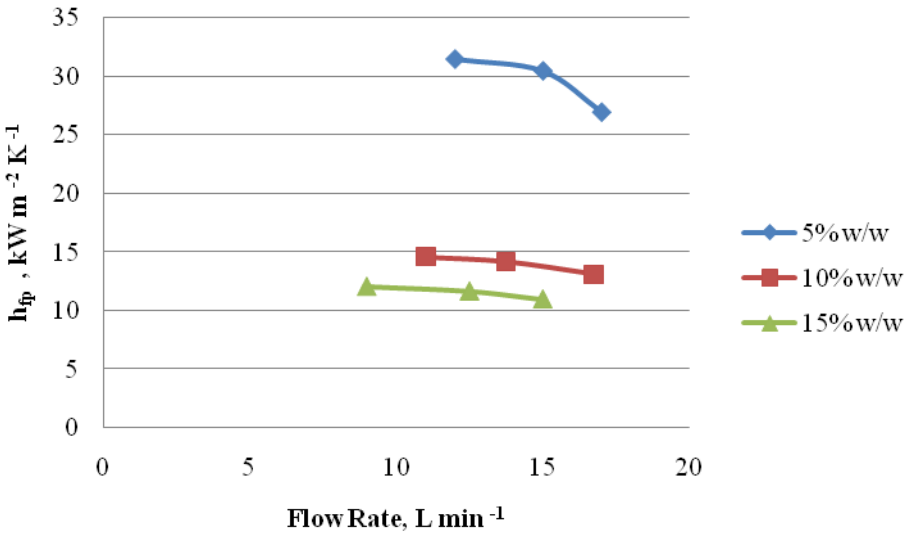

Figure 5 Plots of h_{fp} values against flow rates of rice-water suspension for different solid fractions

3.2.3 Comparison of fluid-to-partilce heat transfer coefficient between cassava and rice suspension

3.2.3.1 Effect of average product flow rate on h_{fp}

The fluid-to-particle heat transfer coefficient decreases with increase in the flow rate. The avearge velocity of the suspension was calculated in the range of 1.50m/s to 2.13m/s and residence time was calculated in the range of 2s to 1.4s which were very small. The temperature of the fluid at the outlet of the tube goes down as the flow rate increases due to larger mass to be heated at a shorter residence time and the same happens for the particles. The temperature gradient between the fluid and the particle was small for cassavadue to the fact that cassava starch globules were smaller than rice grains accompanied by increased fluid to particle convective heat transfer coefficient according to Equation (2). However, these reasons are valid to a greater extent at the highest flow rate where h_{fp} values were relatively low compared to the cases where the flow rate was lower.

3.2.3.2 Effecet of particle surface area on h_{fp}

The lowest heat transfer coefficient was obtained for rice grains at the highest flow rate. The surface area of single rice grain (23.20mm^2) was nearly three times the cassava globule (7.66 mm^2). So, it is expected that heat transfer coefficient would be greater in magnitude for cassava for identical temperature gradient between the fluid and the particle. However, since single rice grain has larger surface area than the cassava globule,the available total heat transfer surface area is almost same for cassava and rice particles (1000 particles mass is 2.7g for cassava where as the same is 9g for rice resulting in greater number of particles for cassava than rice). This could be the possible reason for no difference in h_{fp} between the two.

3.2.3.3 Effect of particle concentration on h_{fp}

As particle concentration increases, h_{fp} values decrease for both cassava and rice supensions. Mankad et al. (1997) studied fluid-to-particle heat transfer in systems of varying solids fractions over a wide range of slip Reynolds numbers and local solids fraction. For slip Reynolds number above 100, they found that in the system of two particles (1.5 cm diameter) placed 1–5 cm apart, h_{fp} values for all inter-particle distances were up to 25% greater than those for a single particle. In variable voidage bed experiments, they found that for a given local Reynolds number, the Nusselt number increased with decreasing voidage (equivalent to increasing particle concentration). Increasing the delivered solids concentration has two effects: reduction in the thermal mass of the fluid and the increase in the thermal mass of solids and hence the specific surface area of solids available for heat transfers and this also makes the system of lower heat source to sink mass ratioresulting in reduced heat transfer. Since, close to the wall region, almost particle free zone developed, the fluid temperature there could be the same or a little high compared to other zones for the same flow rate for all solids concentrations. It can be inferred that for a particular flow rate, ΔT_g in Equation (2) is smaller for higher fraction solids resulting in lower h_{fp} values.

3.3 Analysis of CFD simulation of solid-liquid two phase flow

The effect of particle concentrationand particle size on particle velocity profiles have been studied in horizontal flow. The particle velocity profiles are displayed by plotting velocity against the radial positions in the tube. In general, no particles were observed in the maximum radius range. In most cases, a film of liquid free of particles were seen close to the wall, an effect similarto that reported by some investigators (Maude et al., 1967). Experiments were conducted and computational fluid dynamics was employed to estimate the liquid and particle velocity profiles, as affected by varying particle concentrations (5%, 10%, 15% w/w) on particle velocity profiles using various particle diameters at different flow rates. The density was found to be as 1250 and 1350 kg/m^3 for rice and cassava respectively.Also particle slip velcoity was estimated for both rice and cassava suspensions.

3.3.1 Liquid phase velocity profile

The velocity profile of the solid-liquid flow in the horizontal pipeline is mainly affected by the composition density, volume fraction, and mean velocity. As a result, the velocity profile of the solid-liquid flow in the cross-sectional area of the pipeline differs from that of single-phase flow. In general, the velocity profile in single-phase flow is symmetric and purely parabolic (for laminar) or plug flow (for turbulent) around the pipe centreline, and liquid density is kept as constant in the cross sectional area of the pipeline. However, in the solid-liquid flow, the velocity profile is asymmetrical around the centreline of pipe. Figures6 and 7 show the velocity profiles of suspension at a particular loading of 10% w/w solid fraction. Water density was 998 kg/m^3, cassava density was 1350 kg/m^3, rice density of 1250 kg/m^3, particle diameter of cassava 1.562 mm and equivalent particle diameter of rice was 2.72 mm where s it has intermediate diameter of 1.82 mm. From Figure6, it is clear that the liquid mean velocities near the walls drop down sharply due to the strong viscous shear stress in the turbulent boundary layer and non-slip boundary condition on the wall. It is also clear that the maximum slurry velocity centre appears at the upper part of the pipeline, not exactly at the centreline.

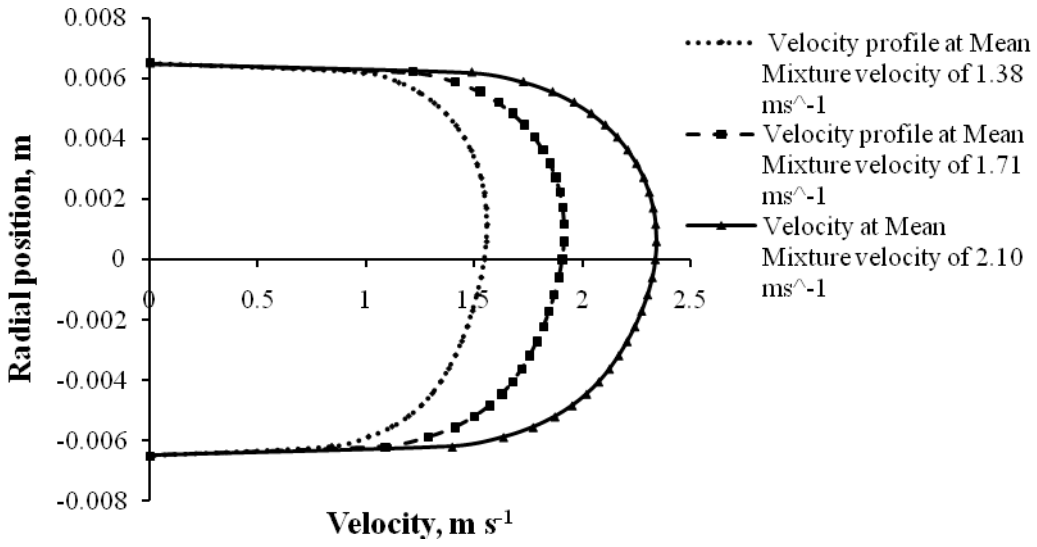

Figure 6 Velocity profile along the vertical diameter at a particular cassava particle concentration (10% w/w)

Figures 6 and 7 also show that the suspension velocity profiles are asymmetric in the vertical direction and the velocity profiles in the lower part of the pipe centreline would be lower than those in the upper part (although it is not very apparent). This occurs because the density of the solid particles is usually greater than that of the liquid; the slurry density in the lower part of the pipe centreline should be greater than those in the upper part based on the effect of gravity and more dissipated energy will be consumed to drive particles for water in the lower part. The asymmetric nature of the velocity profile diminishes as the flow rate increases.

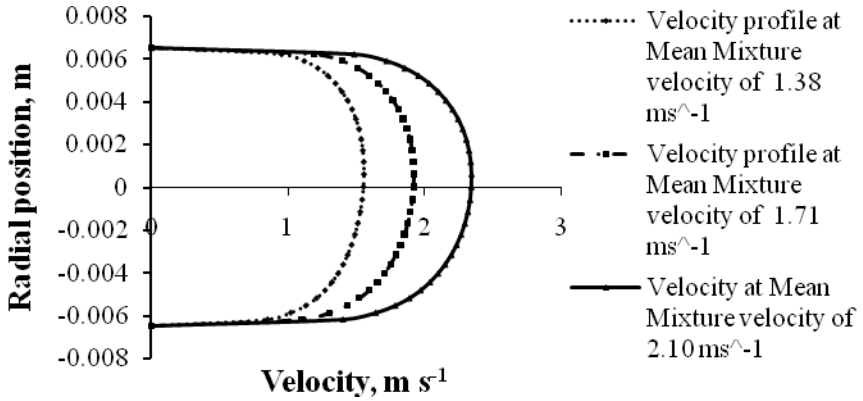

Figure 7 Velocity profile along the vertical diameter at a particular rice particle concentration (10% w/w)

3.3.2. Solid phase velocity profile

The addition of solid particles to turbulent liquid flow modified the velocity distribution of the suspension and the solid phase. Figure8and 9depict the simulated axial velocity profiles along the vertical diameters in fully developed turbulent flow region for solid-liquid flow at different mean mixture velocities.

It is apparent from Figures 8 and 9 that the solid phase velocity profile is generally asymmetrical about the central axis with the particles flowing at higher velocity in

the upper part of the tube than near the base although Figure 9 for rice particle velocity shows symmetrical profile. The profile basically emphasizes 'plug flow. The profiles also show that the particles near the top of the pipe cross-section move faster than the particles at the bottom. Considering the same radial positions, equidistant from the top and the bottom tube wall, particle velocity at the top would be slightly higher than the lower part. Such asymmetric profiles have also been reported for sand and water slurries (Newitt et al., 1962).

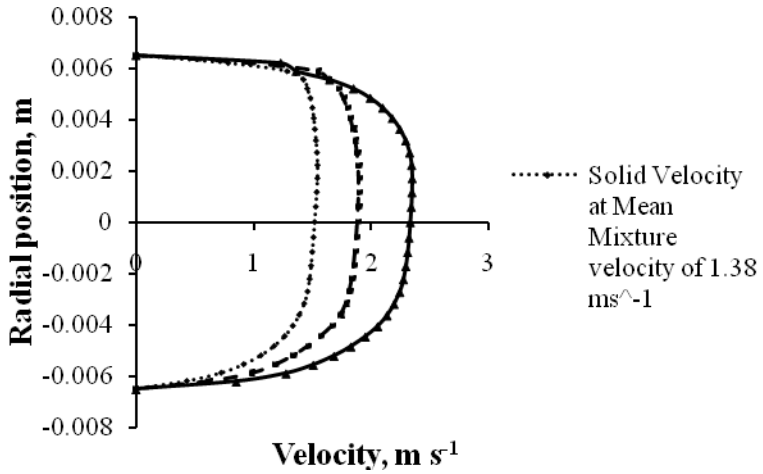

Figure 8 Solid phase velocity profile for cassava-water two phase flows at a particular particle concentration (10% w/w)

The solid phase velocity profile protrudes less in the lower part than in the upper part. This occurs because of the settling tendency of particles due to gravity. With the increase in velocity, the degree of asymmetry of the velocity profile diminishes for both cassava-water and rice-water suspension. The solid phase velocity profile for rice is more symmetrical than cassava. This is because of greater particle density of cassava and their settling down due to the effect of gravity. The degree of asymmetry is also affected by the solids concentration and the particle Reynolds number (Fairhurst et al., 2001; Fairhurst, 1998).

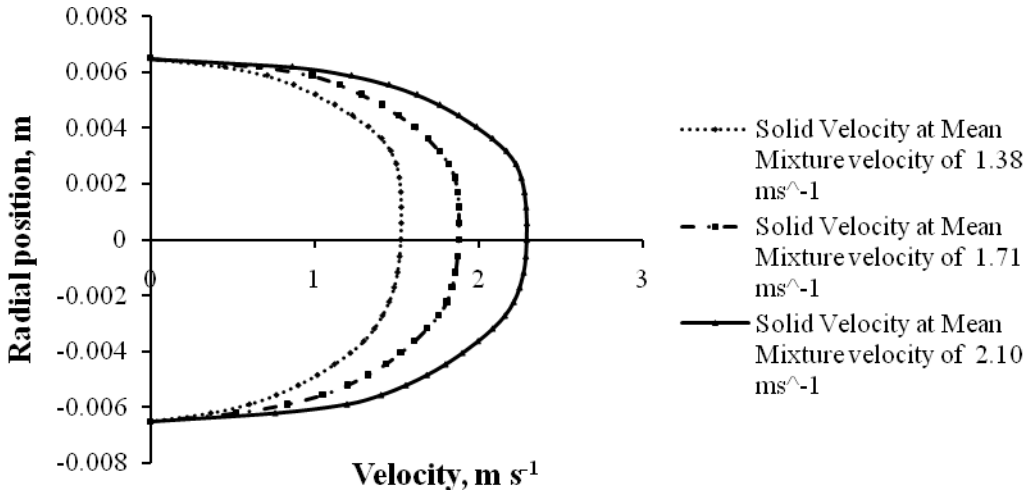

Figure 9 Solid phase velocity profile for rice-water two phase flow at a particular particle concentration (10% w/w)

It has also been observed that the increase in flow rate reduces the bluntness of velocity profile because increase in velocity adds more turbulence which tries to make uniform solid distribution. It is also noteworthy that, except near the bottom, the particles move faster not more than 1.22 times of the mean suspension velocity. This is because (i) the particles can occupy the central region of the pipe (ii) the particles can migrate into faster moving region. Plug flow nature appears for solid phase velocity. This may be because particles near central region of pipe are moving virtually with plug flow.

3.3.3 Particle slip velocity

Slip velocity between liquid and particle can be defined as the difference between liquid velocity and particle velocity over the vertical diameter of the tube. The magnitude of water and particle velocity was obtained from CFD analysis using FLUENT. Slip velocity was estimated across the tube flow which was to be considered as fully developed turbulent flow. The liquid and the particle velocities were estimated separately and the difference between them at different radial positions represents the slip velocity at that particular radius.

3.3.3.1 Slip velocity of cassava particle

Figure 10(a, b and c) shows the particle slip velocity profiles over the vertical centreline of the tube. The profile shown here is asymmetric along the vertical centreline. It clearly shows that slip velocity magnitude is higher near the tube wall. Then it gradually reduces and becomes negative in certain regions and then again increases at the central region. Slip velocity is zero at the wall because of non-slip boundary condition. The particles just adjacent to the boundary wall moves much slower than the liquid resulting in positive slip velocity.

As a general trend, slip velocity close to the centre line increased as particle size increased. However, at larger radius slip velocity varied significantly and became negative near the tube wall. This is possibly due to the fact that higher density solid momentum exceeded that of the liquid where shear rate of the liquid decreased significantly resulting in negative slip velocity (the particle moves faster than the liquid). Slip velocity became positive or almost zero at the central region of pipeline where particles were seen close to the centre line. It implies that the particles move slower than the liquid at the central part. Also the particle concentration is high forming central core around the centre line of the tube. The upper part of the tube has fairly low concentration of particles. It has also been observed that the lower part has also low volume fraction compared to the central region but higher than the upper part. So, particles can move faster in the upper and below the annular core except near-wall region since particles are of small size.

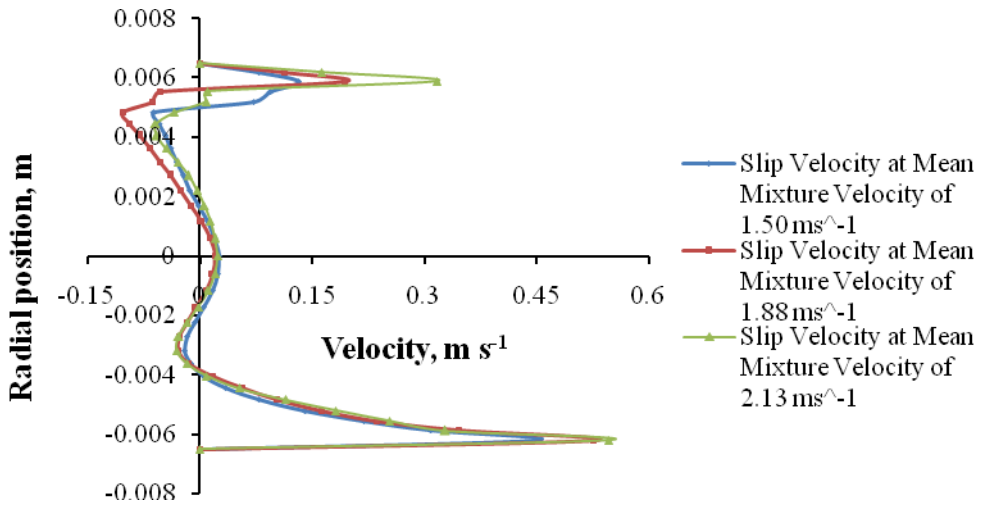

(a) 5% w/w

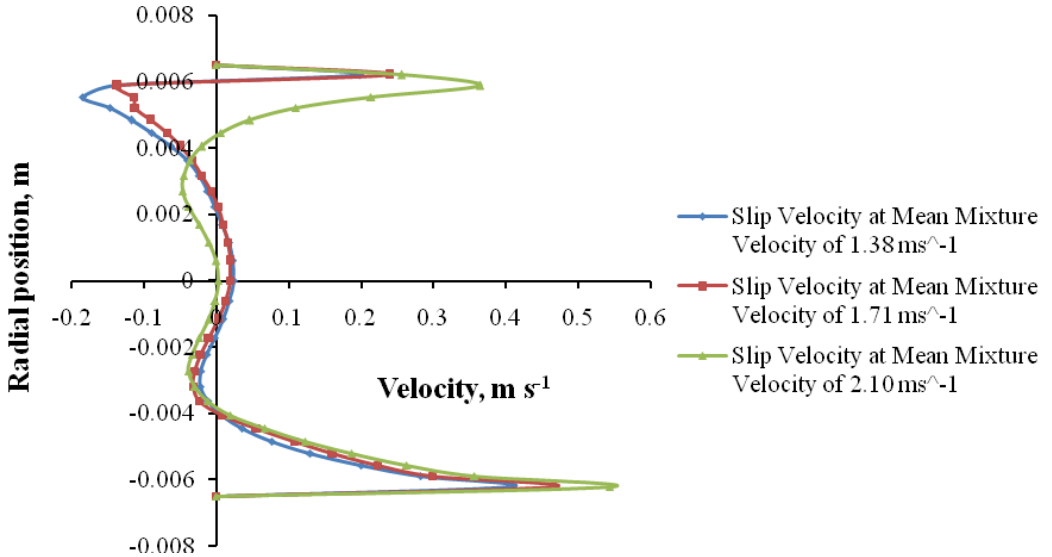

(b) 10% w/w

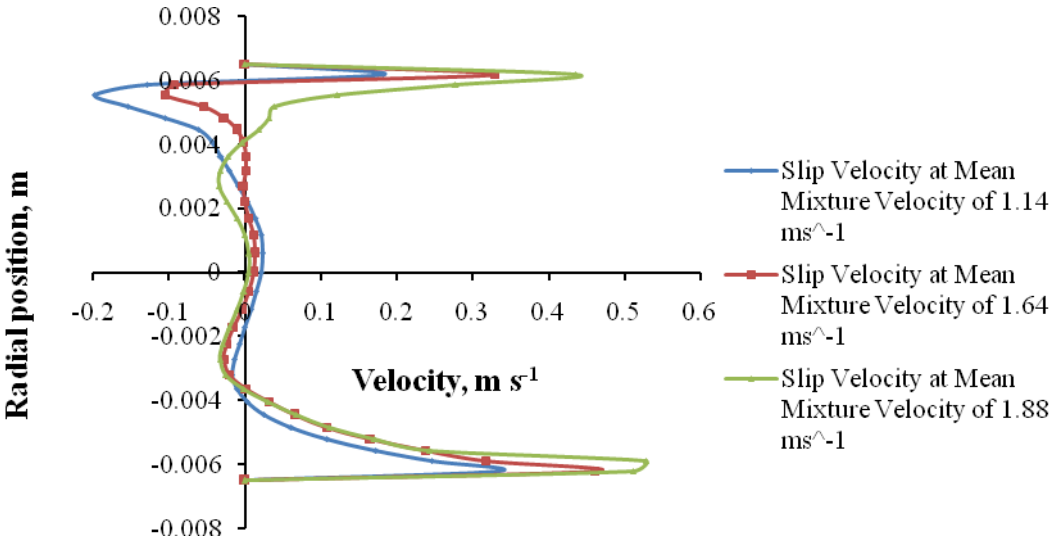

(c) 15% w/w

Figure 10 Slip velocity profiles of cassava for different particle concentrations

3.3.3.2 Slip velocity of rice particle

Figure11 (a, b and c) depicts the slip velocity profile for rice particles along the vertical centreline of the tube. The profile appears to be almost symmetrical about the vertical line. It clearly shows the slip velocity magnitude adjacent to the wall is high while rest of the part gradually decreases becoming small at the central region. (About 2 mm around the tube axis) The average slip velocity over the vertical line obtained was greater for greater flow rate. It has been found in many literatures. At d (particle diameter)= 2mm, the velocity profile is nearly symmetrical (Eesa and Barigou, 2009).

As the particle concentration increases, the slip velocity also increases. Increase in particle concentration makes the solid phase more homogeneous so the particle distribution would be uniform during the flow. But here the concentration distribution has been observed over the tube domain as similar to that of cassava. The particle volume concentration is quite similar around 3.5 mm to 4 mm of the centre line and the particles move slowly compared to the liquid. This is because of lower mass density of rice grains and larger diameter than cassava globules. As diameter increases, tendency of the particle slowing down increases as effective cross sectional area of

fluid flow decreases and hinders the fluid flow. Drag force is needed to push it forward. Absence of negative slip velocity for rice grains compared to cassava is likely due to the fact that the shape of long rice grains allow for streamlined motion entrainment by the liquid and the grains just 'float' along the liquid.

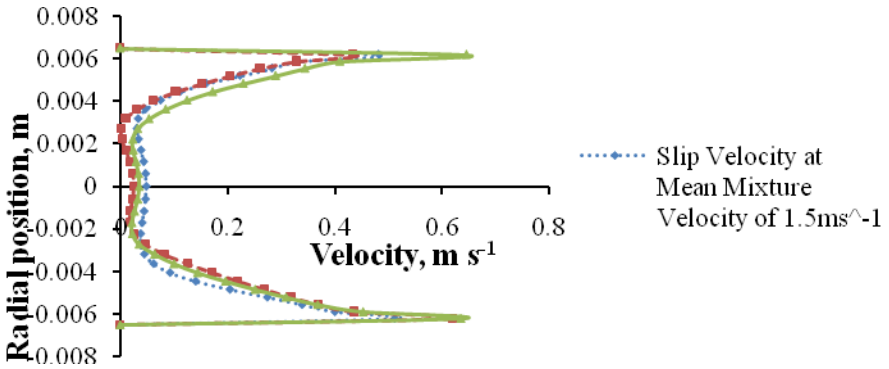

(a) 5% w/w

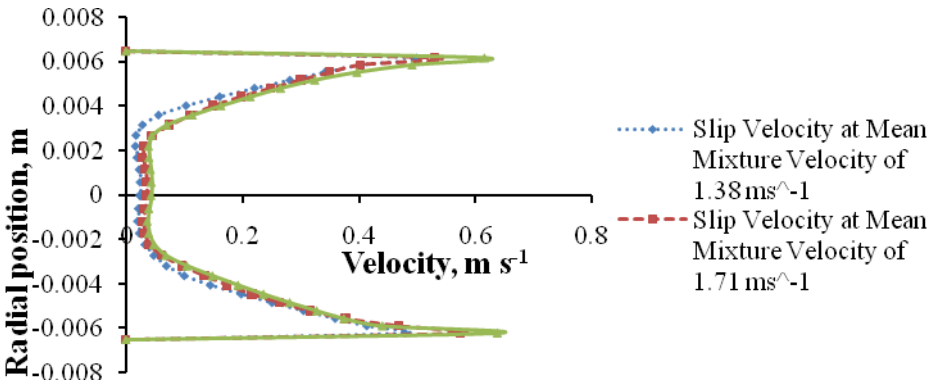

(b) 10% w/w

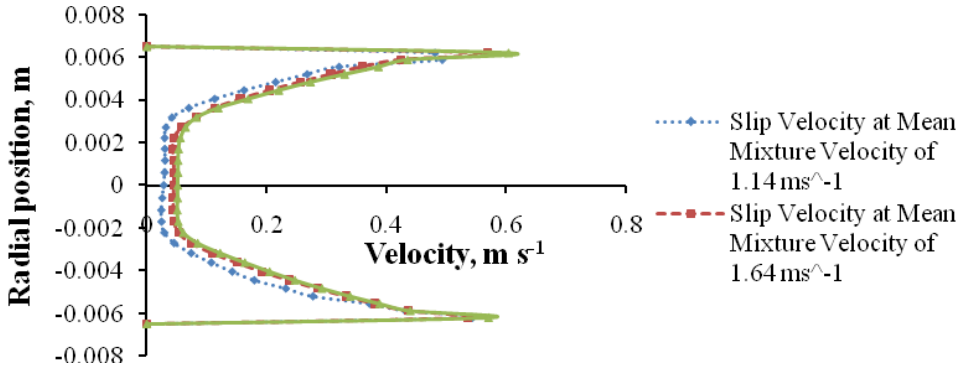

(c) 15% w/w

Figure 11 Slip velocity profiles of rice for different particle concentrations

3.3.4 Solid concentration profile and particle migration

Because concentration profiles depend on many parameters, including suspension velocity, pipe diameter, particle size, and particle density, it is important to test the ability of a model to predict these profiles. Additionally, the knowledge of solids distribution across the pipe cross-section is essential in the evaluation or prediction in straight holding tubes. In this experiment, it is difficult to measure the volume fractions at any point of the pipe cross-sectional area, but it is easy to obtain them in

numerical investigation. Particle volume fraction becomes smaller towards increasing radii forming almost a particle free layer near the tube wall. This is possible due to the absence of outwards inertial effect. The presence of annulus is not apparent. Certain researchers observed a form of concentric flow characterised by a slow moving annulus close to the tube wall and a faster flowing central region.

4 Conclusions

The results of the experiments conducted on particulate flow of cassava – water and rice – water suspensions were in agreement with fundamentals of convective heat transfer as applied from the principles of hydro-thermodynamics to two phase flow and as evidenced in the literature. Developed heat transfer model and CFD analysis were in agreement with basic understanding of heat transfer in two phase flow. Effects of particle geometry were also in agreement with previously reported results in the literature. A detailed insight into various characteristics of two phase flow of grain – water suspension was obtained by application of CFD. The reader is reminded here that the results presented in this article are only the foundation towards optimal design of process heat exchangers which can impart adequate bacterial inactivation combined with preservation of essential nutrients during thermal processing.

NOMENCLATURE

A_i Inside heat exchange area of the surface, m^2

A_p Surface area of each particle, m^2

C_{pg} Specific heat capacity of the grain, kJ kg^{-1} K^{-1}

C_{pw} Specific heat capacity of water, kJ kg^{-1} K^{-1}

D Diameter of the tube, m

D_p Geometric mean diameter of the particle, m

ε Dissipative turbulent kinetic energy, W/m^3

G_b Turbulence kinetic energy due to buoyancy, W/m^3

G_k Turbulence kinetic energy, W/m^3

h Convective wall-to-liquid film heat transfer coefficient, W m^{-2} K^{-1}

h_{fp} Convective fluid to particle heat transfer coefficient, W m^{-2} K^{-1}

$H_{1/2/3\ \varepsilon}$ Constants, dimensionless

κ Turbulent kinetic energy, J/kg^1

L_e Entrance length, m

μ_f Coefficient of viscosity of the fluid, kg m^{-1} s^{-1}

Pr_κ Turbulent Prandtl number, dimensionless

Pr_ε Prandtl Number applicable to dissipation of kinetic energy, dimensionless

φ Solid mass fraction in the suspension, dimensionless

Re_s Slip Reynolds Number, dimensionless

Re_t Tube Reynolds Number, dimensionless

ρ_f Fluid density, kg/m^3

ρ_m Density of the suspension, kg/m^3

$S_{\kappa/\varepsilon}$ User-defined source terms, W/m^3

ΔT Temperature difference between the particle and the fluid, K

ΔT_g Temperature rise of the grain in K

ΔT_{lm} Log-mean temperature difference between the heating medium (steam) and the bulk liquid in K

ΔT_w Temperature rise of the water, K

v_f Fluid velocity, m/s

v_m Mean flow velocity, m/s

v_p Particle velocity, m/s

Y_M Contribution of the fluctuating dilatational incompressible turbulence to the overall dissipation rate, W/m^3

References

Agarwal, P. K. 1988. Transport phenomena in multi-particle systems II. Particle-fluid heat and mass transfer. *Chemical Engineering Science*, 43(9): 2501-2510.

Baptista, P. N., F. A. R.Oliveira, J. C.Oliveira, and S. K.Sastry. 1997. Dimensionless analysis of fluid-to-particle heat transfers coefficients. *Journal of Food Eng*ineering, 31(2 199-218.

Dutta, B. and S. K.Sastry.1990a.Velocity distributions of food particle suspensions in holding tubes: experimental and modelling studies on average particle velocities.*Journal of Food Science*, 55(5): 1448-1453.

Dutta, B. and S. K.Sastry. 1990b. Velocity distributions of food particle suspensions in holding tubes: distribution characteristics and fastest particle velocities. *Journal of Food Science*, 55(6): 1703-1710.

Eesa, M. and M.Barigou. 2009. CFD investigation of the pipe transport of coarse solids in laminar power law fluids. *Chemical Engineering and Science*, 64(2): 322-333.

Eesa, M.and M.Barigou. 2008. Horizontal laminar flow of coarse nearly-neutrally buoyant particles in non-Newtonian conveying fluids: CFD and PEPT experiments compared. *International Journal of Multiphase Flow*, 34 (11): 997–1007.

Fairhurst, P.G., M. Barigou, P.J. Fryer, J.P. Pain, , and D.J Parker . 2001. Using positron emission particle tracking (PEPT) to study nearly neutrally buoyant particles in high solid fraction pipe flow. *International Journal of Multiphase Flow*, 27(11): 1881–1901.

Fairhurst, P.G. 1998. Contribution to the study of the flow behaviour of large nearly neutrally buoyant spheres in non-Newtonian media: application to HTST processing, Ph.D. diss., Universit é de Technologie de Compi ègne, France.

Kelly, B. P., T. R. A. Magee, and M. N. Ahmad . 1995. Convective heat transfer in open channel flow Effects of geometric shape and flow characteristics. *Transactions of the Institute of Chemical Engineering*, 73(C4): 171-182.

Krampa-Morlu, F.N., D.J. Bergstrom, , J.D. Bugg, , R.S.Sanders, and, J. Schaan, 2004. Numerical simulation of dense coarse particle slurry flows in a vertical pipe, In: *Proceedings of the Fifth International Conference on Multiphase Flow*, ICMF'04, Paper No. 460.

Liu, S., J. P. Pain, and P. J Fryer, . 1992. Ecoulement et profiles de vitesse de particules dans les liquides: application aux proceÂdes agro alimentaires. *Entropie*, 28(170): 50-57.

Mankad, S., K. M. Nixon, and P. J. Fryer, 1997. Measurements of particle-liquid heat transfer in systems of varied solids fraction. *Journal of Food Engineering*, 31(1): 9-33.

Maude, A. D., and J. A. Yearn, 1967. Particle migrations in suspension flows. *Journal of Fluid Mechanics*, 30(3): 601-621.

Newitt, D. M., J. F. Richardson, and C. A. Shook, 1962. Hydraulic conveying of solids in horizontal pipes, Part II: Distribution of particles and slip velocities, In *Proceedings*: *Interaction between fluids and particles*, IChemE, London, 87-100.

Ramaswamy, H.S. and M.R. Zareifard, 1999. A Calorimetric approach for evaluation of fluid-to-particle heat transfer coefficient under tube flow Conditions. *Lebensm.-Wiss. u.-Technol.*, 32(8): 495-502.

Ranz, W. E. and W. R. Marshall, 1952a. Evaporation from drops. *Chemical Engineering Progress*, 48(3): 141-146.

Ranz, W. E. and W. R. Marshall, 1952. Evaporation from drops. *Chemical Engineering Progress*, 48 (4): 173-180.

Singh, R. K. and K. Chakrabandhu, 2002. Fluid-to-particle heat transfer coefficients for continuous flow of suspensions in coiled tube and straight tube with bends. *Lebensm.-Wiss. u.-Technol.*, 35(5): 420–435.

Sumner, R.J., M.J. McKibben, and, C.A. Shook, 1990. Concentration and velocity distributions in turbulent vertical slurry flows. *Ecoulements Solide–Liquide*, 2 (2): 33–42.

Tucker, G. S. and P. M. Withers, 1994. Determination of residence time distribution of non-settling food particles in viscous food carrier fluids using Hall Effect sensors. *Journal of Food Process Engineering*, 17(4): 401-422.